

Measuring the 3D Clustering of Undetected Galaxies Through Cross Correlation of their Cumulative Flux Fluctuations from Multiple Spectral Lines

Eli Visbal^{1,2,*} and Abraham Loeb^{2,†}

¹*Jefferson Laboratory of Physics, Harvard University, Cambridge, MA 02138*

²*Harvard-Smithsonian CfA, 60 Garden Street, Cambridge, MA 02138*

(Dated: October 21, 2010)

Abstract

We discuss a method for detecting the emission from high redshift galaxies by cross correlating flux fluctuations from multiple spectral lines. If one can fit and subtract away the continuum emission with a smooth function of frequency, the remaining signal contains fluctuations of flux with frequency and angle from line emitting galaxies. Over a particular small range of observed frequencies, these fluctuations will originate from sources corresponding to a series of different redshifts, one for each emission line. It is possible to statistically isolate the fluctuations at a particular redshift by cross correlating emission originating from the same redshift, but in different emission lines. This technique will allow detection of clustering fluctuations from the faintest galaxies which individually cannot be detected, but which contribute substantially to the total signal due to their large numbers. We describe these fluctuations quantitatively through the line cross power spectrum. As an example of a particular application of this technique, we calculate the signal-to-noise ratio for a measurement of the cross power spectrum of the OI(63 μm) and OIII(52 μm) fine structure lines with the proposed Space Infrared Telescope for Cosmology and Astrophysics (SPICA). We find that the cross power spectrum can be measured beyond a redshift of $z = 8$. Such observations could constrain the evolution of the metallicity, bias, and duty cycle of faint galaxies at high redshifts and may also be sensitive to the reionization history through its effect on the minimum mass of galaxies. As another example of this technique, we calculate the signal-to-noise ratio for the cross power spectrum of CO line emission measured with a large ground based telescope like the Cornell Caltech Atacama Telescope (CCAT) and 21-cm radiation originating from hydrogen in galaxies after reionization with an interferometer similar in scale to the Murchison Widefield Array (MWA), but optimized for post-reionization redshifts.

*visbal@fas.harvard.edu

†aloeb@cfa.harvard.edu

I. INTRODUCTION

Atoms and molecules in the interstellar medium of galaxies produce line emission at particular rest frame wavelengths [1]. For galaxies at cosmological distances, this line emission is redshifted by a factor of $(1+z)$ due to the expansion of the universe. Ignoring peculiar velocities, the redshift of a galaxy corresponds to its distance from the observer along the line of sight. Thus, if the redshift and angular position of many galaxies are measured, a 3D map of their distribution can be constructed. Such 3D maps contain a wealth of information about galaxies and the underlying cosmic density field which they trace. Examples of recent galaxy surveys include the Sloan Digital Sky Survey [2], the 2dF Galaxy Redshift Survey [3], the DEEP2 Redshift Survey [4], and the VIMOS-VLT Deep Survey [5].

In this work, we discuss a different way of mapping the large scale structure of the universe, namely by measuring the fluctuations in line emission from galaxies, including also those too faint to be individually detected. If the line emission fluctuations in observed frequency and angle are associated with a particular line, they can be translated into a 3D map. Even though individual faint sources cannot be distinguished from noise, the cumulative emission from many such sources contributes substantially to the fluctuations over large scales. These fluctuations will trace the large scale structure of the universe and can be analyzed statistically. By contrast, a traditional galaxy survey only contains the positions of galaxies detected at high significance, and discards information from fainter sources.

Similar observations are being planned with the 21cm line of neutral hydrogen using instruments such as MWA [6], LOFAR [7], PAPER [8], 21CMA [9], and SKA [10]. These experiments will obtain angle and frequency information for large areas on the sky and will produce 3D maps of the neutral hydrogen throughout the universe. The raw signal will contain both bright sources of foreground emission (the largest being synchrotron emission from our galaxy), as well as the cosmological 21cm line signal. Since the cosmological signal varies rapidly with frequency, it is expected that the foregrounds, which are smooth in the frequency direction, can be subtracted off [11–14]. If this is accomplished, one will be left with only the fluctuations in 21cm line emission.

During the epoch of reionization the 21cm signal originates from the neutral hydrogen in the intergalactic medium. HII regions ionized by stars or quasars will appear as bubbles in the signal, creating a “Swiss cheese” topology. On the other hand, the post-reionization 21cm signal is expected to originate from dense galactic regions which are self-shielded from the ultraviolet background [15, 16]. Thus, the post-reionization signal is very similar to other galactic emission lines. Recently, statistical analysis of the post-reionization 21cm signal has been attempted [17]. Another idea related to the present work is the cross correlation of the 21cm line with the 92cm line of deuterium [18].

One important issue which does not arise in 21cm observations is confusion from multiple lines. With multiple lines of different rest frame wavelengths the intensity at a particular observed frequency corresponds to emission from multiple redshifts, one for each emission line. With both angle and frequency information, the total emission corresponds to a superposition of 3D maps of galaxies at different redshifts.

Fortunately, it is possible to statistically isolate the fluctuations from a particular redshift by cross correlating the emission from two different lines. If one compares the fluctuations at two different frequencies, which correspond to the same redshift in two different emission lines, their fluctuations will be strongly correlated. However, the signal from any other lines

arises from galaxies at different redshifts which are very far apart and thus will have much weaker correlation.

We propose observations of these cross correlations, and show that they can be described quantitatively by the cross power spectrum of line emission. This technique is particularly suitable for learning about a large sample of faint sources which in a reasonable amount of time can only be detected statistically. As an illustrative example, we calculate the signal-to-noise ratio of the line cross power spectrum which could be measured by the proposed Space Infrared Telescope for Cosmology and Astrophysics (SPICA) [19]. We find that with SPICA, our technique can potentially probe line emission from faint galaxies beyond a redshift $z = 8$. This would contain information about the evolution of distant galaxies including their metallicity, bias and duty cycle. Such observations could also potentially constrain the reionization history based on the minimum mass of galaxies. As another example, we consider cross correlating CO line emission observed with the Cornell Caltech Atacama Telescope (CCAT) [20] and 21cm radiation from galaxies measured by an interferometer similar in scale to the Murchison Widefield Array (MWA) [6], but optimized for post-reionization redshifts.

The paper is organized as follows. In §2 we introduce and describe the 3D line cross power spectrum technique. In §3 and §4 we discuss SPICA and CCAT plus our MWA-like interferometer respectively, which we use to use illustrate the effectiveness of the proposed technique. Finally, we discuss and summarize our conclusions in §5. Throughout, we assume a Λ CDM cosmology with $\Omega_\Lambda = 0.73$, $\Omega_m = 0.27$, $\Omega_b = 0.0456$, $h = 0.7$, and $\sigma_8 = 0.81$ [21].

II. METHOD

A. Line cross power spectrum

We begin by introducing the cross power spectrum of line emission. We assume an observation that records both spatial and spectral data over a patch of the sky. We further assume that the spectrally smooth foreground, including galaxy continuum emission can be subtracted accurately. This could be done by fitting a smooth function of frequency to the data in different locations on the sky as has been suggested for 21cm observations [11–14]. Subtracting such a fit from the data would remove only the signal which varies slowly as a function of frequency. If we associate the fluctuations with emission in a particular line, we can map each pixel to a location in redshift space.

The fluctuation signal at a particular angle on the sky and observed frequency, $\Delta S(\theta_1, \theta_2, \nu) = S(\theta_1, \theta_2, \nu) - \bar{S}$, will have several different components,

$$\Delta S_1(\theta_1, \theta_2, \nu) = \Delta S_{\text{line1}} + \Delta S_{\text{noise}} + \Delta S_{\text{badline1}} + \Delta S_{\text{badline2}} + \Delta S_{\text{badline3}} + \dots \quad (1)$$

These include fluctuations in line emission from galaxies at the target redshift in the associated line, detector noise, and emission from galaxies at different redshifts in other lines. We term these “bad lines”.

To estimate the flux amplitude of line emission fluctuations we assume that galaxies trace the underlying cosmological density field. If we consider linear scales, it follows that the line fluctuations due to galaxy clustering are given by $\Delta S = \bar{S} \bar{b} \delta(\mathbf{r})$, where \bar{S} is the average line signal, \bar{b} is the luminosity weighted average galaxy bias, and $\delta(\mathbf{r})$ is the cosmological over-density at a location \mathbf{r} corresponding to the observed angle and frequency. For the

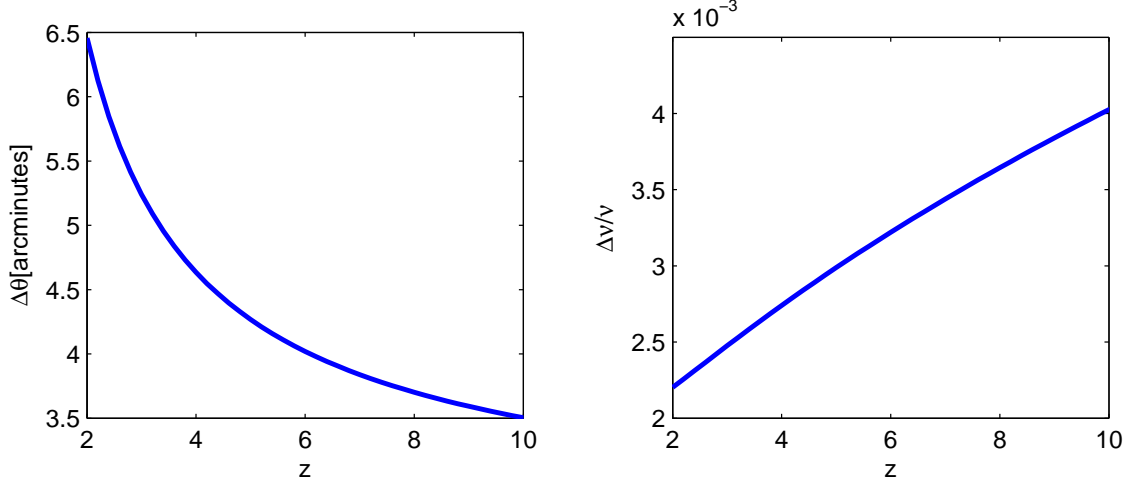


FIG. 1: The angle and frequency range corresponding to 10 comoving Mpc.

moment we ignore Poisson fluctuations due to the discrete nature of galaxies, which will be introduced later. We describe our method for estimating the average signal and bias of emission lines in the next subsection.

Ignoring peculiar velocities and using the flat sky approximation (which applies for the small fields of view we consider in this paper), we find,

$$\Delta S_{\text{line1}} = \bar{S}_1 \bar{b} \delta(\mathbf{r}_o + \Delta\theta_1 D_A \hat{\mathbf{i}} + \Delta\theta_2 D_A \hat{\mathbf{j}} + \Delta\nu \tilde{y}_1 \hat{\mathbf{k}}), \quad (2)$$

where \mathbf{r}_o is the comoving position corresponding to the center of the survey, $\Delta\theta_1$ and $\Delta\theta_2$ are the angular offsets from the center of the survey and $\Delta\nu$ is the offset from the central observed frequency, D_A is the angular diameter distance in comoving units, and \tilde{y} is the derivative of comoving distance with respect to observed frequency. This last quantity is given by,

$$\tilde{y} = \frac{d\chi}{d\nu} = \frac{d\chi}{dz} \frac{dz}{d\nu} = \frac{\lambda_r (1+z)^2}{H(z)}, \quad (3)$$

where χ is the comoving distance to the observation, ν is the observed frequency, λ_r is the rest frame wavelength of a line, and $H(z)$ is the Hubble parameter. Here $\hat{\mathbf{i}}$, $\hat{\mathbf{j}}$, and $\hat{\mathbf{k}}$ are Cartesian unit vectors with $\hat{\mathbf{k}}$ pointing along the line of sight of the survey. In Figure 1 we show the relation between angle, frequency, and comoving position as a function of redshift.

Similarly, for the bad lines we have,

$$\Delta S_{\text{badline1}} = \bar{B}_1 \bar{b}_1 \delta(\mathbf{r}_o + d_1 \hat{\mathbf{k}} + \Delta\theta_1 D_{A1} \hat{\mathbf{i}} + \Delta\theta_2 D_{A1} \hat{\mathbf{j}} + \Delta\nu \tilde{y}_{b1} \hat{\mathbf{k}}), \quad (4)$$

where d_1 is the shift along the line of sight due to each bad line being at a different redshift than the target line, \bar{B}_1 is the average signal from the bad line, and \bar{b}_1 is the average bias of the galaxies emitting in the bad line. Note that the angular diameter distance and derivative of comoving distance with respect to observed frequency are evaluated at the redshift of the bad line galaxies which we denoted with subscripts.

Instead of angle and frequency we label our observed pixels in terms of the location in space corresponding to our target line (\mathbf{r}_o, \mathbf{r}), where $\mathbf{r} = x\hat{\mathbf{i}} + y\hat{\mathbf{j}} + z\hat{\mathbf{k}}$ is the distance from

the center of the survey, with $x = \Delta\theta_1 D_A$, $y = \Delta\theta_2 D_A$, and $z = \Delta\nu\tilde{y}$. We rewrite Eq. (1) using these coordinates,

$$\Delta S_1(\mathbf{r}_o, \mathbf{r}) = \Delta S_{\text{noise}} + \bar{S}_1 \bar{b} \delta(\mathbf{r}_o + \mathbf{r}) + \bar{B}_1 \bar{b}_1 \delta(\mathbf{r}_o + d_1 \hat{\mathbf{k}} + \mathbf{r}'_1) + \bar{B}_2 \bar{b}_2 \delta(\mathbf{r}_o + d_2 \hat{\mathbf{k}} + \mathbf{r}'_2) + \dots, \quad (5)$$

where $\mathbf{r}'_n = c_{xn}x\hat{\mathbf{i}} + c_{yn}y\hat{\mathbf{j}} + c_{zn}z\hat{\mathbf{k}}$ for the n 'th bad line. The constants c_{xn} , c_{yn} and c_{zn} reflect the cosmological stretching of the data cube at different redshifts, which are given by $c_{xn} = c_{yn} = D_{An}/D_A$ and $c_{zn} = \tilde{y}_{bn}/\tilde{y}_1$.

As mentioned in the Introduction, we can statistically remove the contribution from bad lines by cross correlating the fluctuations from two different lines originating from nearby locations. We define the 2-point cross correlation function as,

$$\xi_{1,2}(\mathbf{r}) = \langle \Delta S_1(\mathbf{r}_o, \mathbf{x}) \Delta S_2(\mathbf{r}_o, \mathbf{r} + \mathbf{x}) \rangle, \quad (6)$$

and the cross correlation power spectrum as its Fourier transform,

$$P_{1,2}(\mathbf{k}) = \int d^3\mathbf{r} \xi_{1,2}(\mathbf{r}) e^{i\mathbf{k}\cdot\mathbf{r}}. \quad (7)$$

Note that the noise in different pixels will be uncorrelated and that bad line emission from different lines will in general originate from galaxies at different redshifts which will be essentially uncorrelated. Thus, we expect the cross correlation function and power spectrum to depend only on galaxies at the target location,

$$\xi_{1,2}(\mathbf{r}) = \langle \Delta S_{\text{line1}}(\mathbf{r}_o, \mathbf{x}) \Delta S_{\text{line2}}(\mathbf{r}_o, \mathbf{r} + \mathbf{x}) \rangle = \bar{S}_1 \bar{S}_2 \bar{b}^2 \langle \delta(\mathbf{x}) \delta(\mathbf{r} + \mathbf{x}) \rangle = \bar{S}_1 \bar{S}_2 \bar{b}^2 \xi(\mathbf{r}), \quad (8)$$

where $\xi(\mathbf{r})$ is the cosmological matter correlation function.

B. Average signal, average bias, and shot-noise

To calculate the average signal and bias for a particular line, we assume that the luminosity of a galaxy in a particular line is a function of the mass of the halo hosting it: $L = L(M)$. We also assume that galaxies only emit a significant amount of radiation over some fraction of cosmic time, the duty cycle, ϵ_{duty} . The average signal is then (in erg/s/cm²/Hz/Sr),

$$\bar{S} = \int_{M_{\min}}^{\infty} dM \frac{L(M)}{4\pi D_L^2} \epsilon_{\text{duty}} \frac{dn}{dM} \tilde{y} D_A^2, \quad (9)$$

where M_{\min} is the minimum mass of dark matter halos which can host galaxies, and $dn(M)$ is the comoving density of halos of mass between M and $M + dM$. Before reionization M_{\min} is set by the requirement that gas can cool efficiently via atomic hydrogen cooling, corresponding to halos with virial temperatures greater than 10⁴K, whereas after reionization this is the threshold for assembling heated gas out of the photo-ionized intergalactic medium, corresponding to a minimum virial temperature of 10⁵K [22–29]. $L(M)$ is the line luminosity (in erg/s) from one dark matter halo of mass M , D_L is the cosmological luminosity distance, and $\frac{dn}{dM}$ is the halo mass function in units of comoving density per mass [30].

Assuming that the flux in a line from a halo is proportional to the mass of the halo, the average bias is given by,

$$\bar{b} = \frac{\int_{M_{\min}}^{\infty} \frac{dn}{dM} b(M, z) M dM}{\int_{M_{\min}}^{\infty} \frac{dn}{dM} M dM}, \quad (10)$$

where $b(M, z)$ is the bias associated with halos of mass M at redshift z [30]. We can calculate the average signal and bias for both the target lines and bad lines using Eqs. (9) and (10). Note that both of these quantities must be calculated at the appropriate redshifts for the different bad lines.

In addition to fluctuations due to the clustering of galaxies, there are also Poisson fluctuations arising from the discrete nature of galaxies which sample the cosmological density field. These fluctuations are unimportant on very large scales, but dominate on the smallest scales. Given our model of the line fluctuations, it is straightforward to show from Eqs. (6) and (7) that the cross power spectrum of galaxy line emission from two lines is given by,

$$P_{1,2}(\mathbf{k}) = \bar{S}_1 \bar{S}_2 \bar{b}^2 P(\mathbf{k}) + P_{\text{shot}}, \quad (11)$$

where $P(\mathbf{k})$ is the cosmic power spectrum of density fluctuations and the Poisson or shot-noise power spectrum due to the discrete nature of galaxies is given by,

$$P_{\text{shot}} = \int_{M_{\min}}^{\infty} dM \left(\frac{L_1(M)}{4\pi D_L^2} \right) \left(\frac{L_2(M)}{4\pi D_L^2} \right) \epsilon_{\text{duty}} \frac{dn}{dM} (\tilde{y}_1 D_A^2) (\tilde{y}_2 D_A^2), \quad (12)$$

where the indices 1 and 2 denote lines 1 and 2.

C. Cross power spectrum estimation

Next we introduce an unbiased estimator of the cross power spectrum and use it to derive an expression for the variance in its measurement. We begin by defining the Fourier amplitude of the fluctuations,

$$f_{\mathbf{k}} = \int d^3\mathbf{r} \Delta S(\mathbf{r}_o, \mathbf{r}) W(\mathbf{r}) e^{i\mathbf{k} \cdot \mathbf{r}}, \quad (13)$$

where $W(\mathbf{r})$ is a window function which is constant over the survey volume and zero outside the survey volume. It is normalized such that, $\int W d^3\mathbf{r} = 1$. The center of the survey volume is denoted by \mathbf{r}_o .

The Fourier amplitude can be broken up into the different sources of fluctuations,

$$f_{\mathbf{k}}^{(1)} = f_{\mathbf{k}}^{S1} + f_{\mathbf{k}}^{n1} + f_{\mathbf{k}}^{B1} + f_{\mathbf{k}}^{B2} \dots, \quad (14)$$

the galaxy line fluctuations at the target redshift, detector noise, and each of the bad lines coming from different redshifts.

Using the convolution theorem, we rewrite the Fourier amplitude for the target line fluctuations as,

$$f_{\mathbf{k}}^{S1} = \frac{1}{(2\pi)^3} \int d^3\mathbf{k}' \bar{S}_1 \bar{b} \delta(\mathbf{k}') W(\mathbf{k}' - \mathbf{k}) e^{-i\mathbf{k}' \cdot \mathbf{r}_o}. \quad (15)$$

A rectangular window function in real space has the k-space form,

$$W(k_x, k_y, k_z) = \frac{\sin(k_x a_x/2)}{(k_x a_x/2)} \frac{\sin(k_y a_y/2)}{(k_y a_y/2)} \frac{\sin(k_z a_z/2)}{(k_z a_z/2)}, \quad (16)$$

where a_x , a_y , and a_z are the spatial dimensions of the survey along the x , y , and z axes.

The Fourier amplitude defined above can now be used to estimate the cross power spectrum of different lines. If we cross correlate the Fourier amplitude of two different lines corresponding to the same location, $\langle f_{\mathbf{k}}^{(1)} f_{\mathbf{k}}^{(2)*} \rangle$, all terms except for the target lines' fluctuations are greatly suppressed as discussed above. Ignoring momentarily the fluctuations due to the discrete nature of galaxies, this results in,

$$\langle f_{\mathbf{k}}^{(1)} f_{\mathbf{k}}^{(2)*} \rangle = \frac{1}{(2\pi)^6} \int \int d^3\mathbf{k}' d^3\mathbf{k}'' W(\mathbf{k}' - \mathbf{k}) W(\mathbf{k}'' - \mathbf{k})^* \bar{S}_1 \bar{S}_2 \bar{b}^2 \langle \delta(\mathbf{k}') \delta(\mathbf{k}'')^* \rangle e^{i(\mathbf{k}'' - \mathbf{k}') \cdot \mathbf{r}_0}. \quad (17)$$

Note that the cosmological power spectrum is defined by,

$$\langle \delta(\mathbf{k}') \delta(\mathbf{k}'')^* \rangle = (2\pi)^3 \delta^D(\mathbf{k}' - \mathbf{k}'') P(k'), \quad (18)$$

and that for a large survey $|W(\mathbf{k}' - \mathbf{k})|^2 \approx (2\pi)^3 \delta^D(\mathbf{k}' - \mathbf{k})/V$, where δ^D is a Dirac delta function and V is the volume of the survey. With these substitutions we find that,

$$\langle f_{\mathbf{k}}^{(1)} f_{\mathbf{k}}^{(2)*} \rangle = \bar{S}_1 \bar{S}_2 \bar{b}^2 P(\mathbf{k})/V, \quad (19)$$

which is simply the clustering component of the cross power spectrum divided by the volume of the survey. When Poisson fluctuations due to the discrete nature of galaxies are included it is straightforward to show that this will give the total line cross power spectrum divided by the volume of the survey. Thus, we take our unbiased estimator to be the real part of this quantity times the volume of the survey,

$$\hat{P}_{1,2} = \frac{V}{2} (f_{\mathbf{k}}^{(1)} f_{\mathbf{k}}^{(2)*} + f_{\mathbf{k}}^{(1)*} f_{\mathbf{k}}^{(2)}). \quad (20)$$

Equipped with an estimator, we can now calculate the variance on a measurement of the cross power spectrum. The error is given by,

$$\delta P_{1,2}^2 = \langle \hat{P}_{1,2}^2 \rangle - \langle \hat{P}_{1,2} \rangle^2. \quad (21)$$

With this estimator we find (see appendix A),

$$\delta P_{1,2}^2 = \frac{1}{2} (P_{1,2}^2 + P_{1\text{total}} P_{2\text{total}}), \quad (22)$$

where $P_{1\text{total}}$ is the total power spectrum corresponding to the first line being cross correlated,

$$P_{1\text{total}} = \bar{S}_1^2 \bar{b}^2 P(\mathbf{k}, z_{\text{target}}) + P_{\text{noise}} + \bar{B}_1^2 \bar{b}_1^2 \frac{P(\mathbf{k}'_1, z_1)}{(c_{x1} c_{y1} c_{z1})} + \bar{B}_2^2 \bar{b}_2^2 \frac{P(\mathbf{k}'_2, z_2)}{(c_{x2} c_{y2} c_{z2})} \dots \quad (23)$$

Here we have the total power spectrum for each line, which includes the line fluctuation power spectrum of the line at the target redshift; a power spectrum due to the detector noise fluctuations; and the power spectrum for each of the bad lines. The c 's which appear in the denominators of the bad line power spectra result from the fact that the volume corresponding to the field of view on the sky and frequency interval of the survey is different for the location of each bad line. Similarly, the wave-number for the various bad lines is changed to $\mathbf{k}'_1 = \frac{k_x}{c_{x1}} \hat{\mathbf{i}} + \frac{k_y}{c_{y1}} \hat{\mathbf{j}} + \frac{k_z}{c_{z1}} \hat{\mathbf{k}}$. To avoid an overly cumbersome equation, we have not explicitly written the shot-noise power spectra. Note that for each clustering power spectrum which appears in this equation there is a corresponding P_{shot} given by Eq. (12).

Up to this point we have only been dealing with the error in an estimate of one k-mode. However, one can exploit the isotropy of the universe and average the value of the cross power spectrum for a thin spherical shell in k-space. The error on the cross power spectrum changes as a function of angle in k-space (due to \mathbf{k}' appearing in Eq. 23). One should take a weighted average, where modes in the shell with a better signal-to-noise ratio are weighted more heavily. The optimal way to do this is an inverse variance weighted average of the cross power spectrum in the shell. It follows that the error on the averaged cross power spectrum is given by,

$$\delta P(k)_{1,2} = \left(\sum_{\text{shell}} \frac{1}{\delta P_{1,2}(\mathbf{k})^2} \right)^{-1/2}, \quad (24)$$

where we are summing over all of the modes in a shell. Note that the resolution of k-space is given by $2\pi/a_i$ in the i 'th direction for Cartesian coordinates. We only add modes in the upper half-plane because the power spectrum is the Fourier transform of a real-valued function. The maximum k-modes available are set by the angular and frequency resolution of the observations, while the minimum values are set by the dimensions of the survey volume.

D. Multiple lines

One could also combine the information from the cross correlations of many lines. For instance, one could do a weighted average of the cross power spectra of all combinations of available lines,

$$P_{\text{AVG}} = w_{1,2}\hat{P}_{1,2} + w_{1,3}\hat{P}_{1,3} + w_{2,3}\hat{P}_{2,3} \dots \quad (25)$$

where the w 's are weighting factors which would need to be highest for the pairs of lines with the highest signal-to-noise ratio. This helps to detect the faintest galaxies.

E. Remaining confusion

As discussed above, if one cross correlates fluctuations from two different lines at frequencies corresponding to a target redshift, each will have its own set of bad lines from various other redshifts. If a bad line from the first line originates from a redshift very close to a bad line from the second line there may be a spurious signal in the cross correlation of the fluctuations which is not from the target redshift.

Fortunately, we do not expect this type spurious signal to be very problematic. If a pair of spurious bad lines is present one should be able to cross correlate this pair directly (then the target lines will appear as a spurious pair). As long as the fluctuations from the spurious pair are not much larger than the target lines, one will be able to accurately subtract off their contribution. In the examples with SPICA considered below, we find that after all of the bright sources which can be individually detected are removed, the fluctuations from each bad line are smaller or comparable to the fluctuations in the lines we cross correlate.

A factor which will aid in subtracting off this spurious signal is that (ignoring redshift space distortions), the cross power spectrum from the target lines will only depend on the magnitude of \mathbf{k} and not the direction. However, the signal from the spurious pair will change with the direction of the k-mode due to the stretching of the data cube (i.e. they have different c_x , c_y , and c_z values defined above).

There is an additional effect which will further eliminate this problem. Two problematic bad lines will never originate from exactly the same redshift. Since they are from slightly different redshifts, the 3D data cube corresponding to the location of the emitting galaxies will be stretched by different amounts. That means when we cross correlate the same \mathbf{k} in the target lines they will have slightly different \mathbf{k} values in each of the problematic bad lines. Since k-modes which have different \mathbf{k} are uncorrelated, this will serve to reduce the spurious signal.

III. SPICA

A. Instrument

We use the proposed Space Infrared Telescope for Cosmology and Astrophysics (SPICA) [19] as an example of an instrument which could be used to cross correlate line emission as discussed above. SPICA is a 3.5 meter space-borne infrared telescope planned for launch in 2017. It will be cooled below 5K, providing measurements which are orders of magnitude more sensitive than those from current instruments. We also consider the Atacama Large Millimeter Array (ALMA) [31], but find that it is not well suited for the cross correlations discussed in this paper. Due to the small field of view and high angular resolution of this instrument, after the detectable galaxies have been removed, we find that remaining statistical signal cannot be detected above the detector noise.

We focus on SPICA's proposed high performance spectrometer μ -spec (H. Moseley, private communication 2009). This instrument will provide background limited sensitivity with wavelength coverage from $250 - 700\mu m$. A number of μ -spec units will be combined to record both angle and spectral data in each pointing, which will be perfectly suited for the cross correlation technique described above. We assume that spectra for 100 diffraction limited pixels can be measured simultaneously with a resolving power of $R = \nu/\Delta\nu = 1000$, this represents an optimistic design. We expect that most of the signal contributed by galaxies which cannot be observed directly will originate from lines too narrow to be resolved with this resolution. We have checked this by associating halos of a given mass with a corresponding rotational velocity.

Since our observations are background limited, the noise fluctuations will be dominated by shot-noise from the finite number photons originating from the smooth foregrounds which we assume have been subtracted off. In the wavelength range considered, the dominant foregrounds are dust emission from the Milky Way galaxy and zodiacal light from the solar system. We use COBE FIRAS data to estimate the brightness of the total foregrounds in the faintest 10% region of the sky [32]. If the observation has pixels with solid angle $\Delta\Omega$ and frequency width $\Delta\nu$, the foreground flux fluctuations (in $\text{erg/s/cm}^2/\text{Sr/Hz}$) in one pixel will be,

$$\Delta S_{\text{noise}} = \frac{E_\gamma}{At\Delta\Omega\Delta\nu}(N_\gamma - \bar{N}_\gamma), \quad (26)$$

where E_γ is the energy per photon coming from the foreground, A is the area of the primary dish of the telescope, t is the integration time, N_γ is the number of photons gathered in a pixel during the integration time, and \bar{N}_γ is the average number of photons that are collected from one pixel during the integration time. From Poisson statistics it follows that

the variance due to the foregrounds in a pixel is given by,

$$\sigma_{\text{noise}}^2 = \frac{\bar{S}_{\text{fg}} E_{\gamma}}{At \Delta \Omega \Delta \nu}, \quad (27)$$

where \bar{S}_{fg} is the average surface brightness from the foregrounds (in $\text{erg/s/cm}^2/\text{Sr/Hz}$). One can then derive (see appendix A) the noise power spectrum,

$$P_{\text{noise}} = \bar{S}_{\text{fg1}} \frac{E_{\gamma} D_A^2 \tilde{y}}{At}. \quad (28)$$

In deriving this equation we have implicitly assumed that the arrival of individual photons are statistically independent from one another. This will be true for foreground radiation at the wavelengths we consider with SPICA. However, at wavelengths longer than $\sim 1\text{mm}$ this assumption might no longer apply. In general, one needs to use the full equation for photon noise which includes correlations from photons arriving in the same quantum state. This correlation in the arrival time of photons, so called “photon bunching”, will increase the noise calculated with simple Poisson statistics for individual photons [33, 34].

B. Relevant lines

Atomic and ionic fine-structure lines in the far infrared are very important in cooling the gas in galaxies. They produce bright emission lines which can be seen in distant sources. For galaxies with redshifts of $z \gtrsim 5$ many of these lines will be observed within SPICA’s wavelength range.

In order to estimate the amplitude of line emission fluctuations we assume a linear relationship between line luminosity, L , and star formation rate, \dot{M}_* . The line luminosity from a galaxy is then given by $L = \dot{M}_* \cdot R$, where R is the ratio between star formation rate and line luminosity for a particular line. This is similar to existing relations in different bands (see [35]) and was used in the past to estimate the strength of the galactic lines [36]. For the first 7 lines in Table I, we use the same ratios, R , as [36] which were calculated by taking the geometric average of the ratios from an observational sample of lower redshift galaxies [37].

We also list line strengths for CO lines which could be observed with other instruments (see §4). For transitions below CO(8-7), we use the same R values as [36], which are calibrated from observations of the galaxy M82 [38]. For the higher CO transitions we calibrate with the observations of M82 presented in Ref. [39]. The R values of M82 are representative of CO emission from high redshift galaxies (see Figure 1 in Ref. [36]).

We calculate the star formation rate in a halo by denoting the fraction of gas in a halo which forms stars as the star formation efficiency, f_* . We then approximate the star formation rate as constant over the duty cycle of the galaxy. Following ([26, 40, 41]) we write,

$$\dot{M}_*(M) = \frac{f_*(\Omega_b/\Omega_m)M}{\epsilon_{\text{duty}} t_H}, \quad (29)$$

where $t_H = 0.97[(1+z)/7]^{-3/2}\text{Gyr}$ is the age of the Universe at the high redshifts of interest. The line luminosity of a galaxy is then given by,

$$L = 6.6 \cdot 10^6 \left(\frac{R}{3.8 \cdot 10^6} \right) \left(\frac{M}{10^{10} M_{\odot}} \right) \left(\frac{1+z}{7} \right)^{3/2} \frac{f_*}{\epsilon_{\text{duty}}} L_{\odot}. \quad (30)$$

TABLE I: Assumed ratio between star formation rate, \dot{M}_* , and line luminosity, L , for various lines. For the first 7 lines this ratio is measured from a sample of low redshift galaxies. The other lines have been calibrated based the galaxy M82. We obtain the luminosity in a line from: $L[L_\odot] = R \cdot \dot{M}_*[M_\odot \text{ yr}^{-1}]$.

Species	Emission Wavelength[μm]	$R[L_\odot/(M_\odot/\text{yr})]$
CII	158	6.0×10^6
OI	145	3.3×10^5
NII	122	7.9×10^5
OIII	88	2.3×10^6
OI	63	3.8×10^6
NIII	57	2.4×10^6
OIII	52	3.0×10^6
CO(1-0)	2610	3.7×10^3
CO(2-1)	1300	2.8×10^4
CO(3-2)	866	7.0×10^4
CO(4-3)	651	9.7×10^4
CO(5-4)	521	9.6×10^4
CO(6-5)	434	9.5×10^4
CO(7-6)	372	8.9×10^4
CO(8-7)	325	7.7×10^4
CO(9-8)	289	6.9×10^4
CO(10-9)	260	5.3×10^4
CO(11-10)	237	3.8×10^4
CO(12-11)	217	2.6×10^4
CO(13-12)	200	1.4×10^4
CI	610	1.4×10^4
CI	371	4.8×10^4
NII	205	2.5×10^5

C. Results

To demonstrate the effectiveness of the cross correlation technique, we calculate the signal-to-noise ratio for the line cross power spectrum of OI($63\mu\text{m}$) and OIII($52\mu\text{m}$) measured with SPICA. Because this technique is most useful for detecting faint galaxies which cannot be individually detected, we assume that all of the pixels containing very bright line emission have been removed. This is done for both the lines we are cross correlating and the bad lines. We assume that all pixels with line emission corresponding to 5σ peaks when compared with the foreground noise are removed. This effectively changes the upper limits of integration in Eqs. (9) and (10). We find that this only requires removing a small fraction of the available pixels. All lines in Table I are used as bad lines.

In order to calculate which dark matter halos are bright enough to be removed, we assume that all of the emission from a halo appears in one pixel. We expect this to be a good approximation, since most of the signal from high redshift galaxies originates in

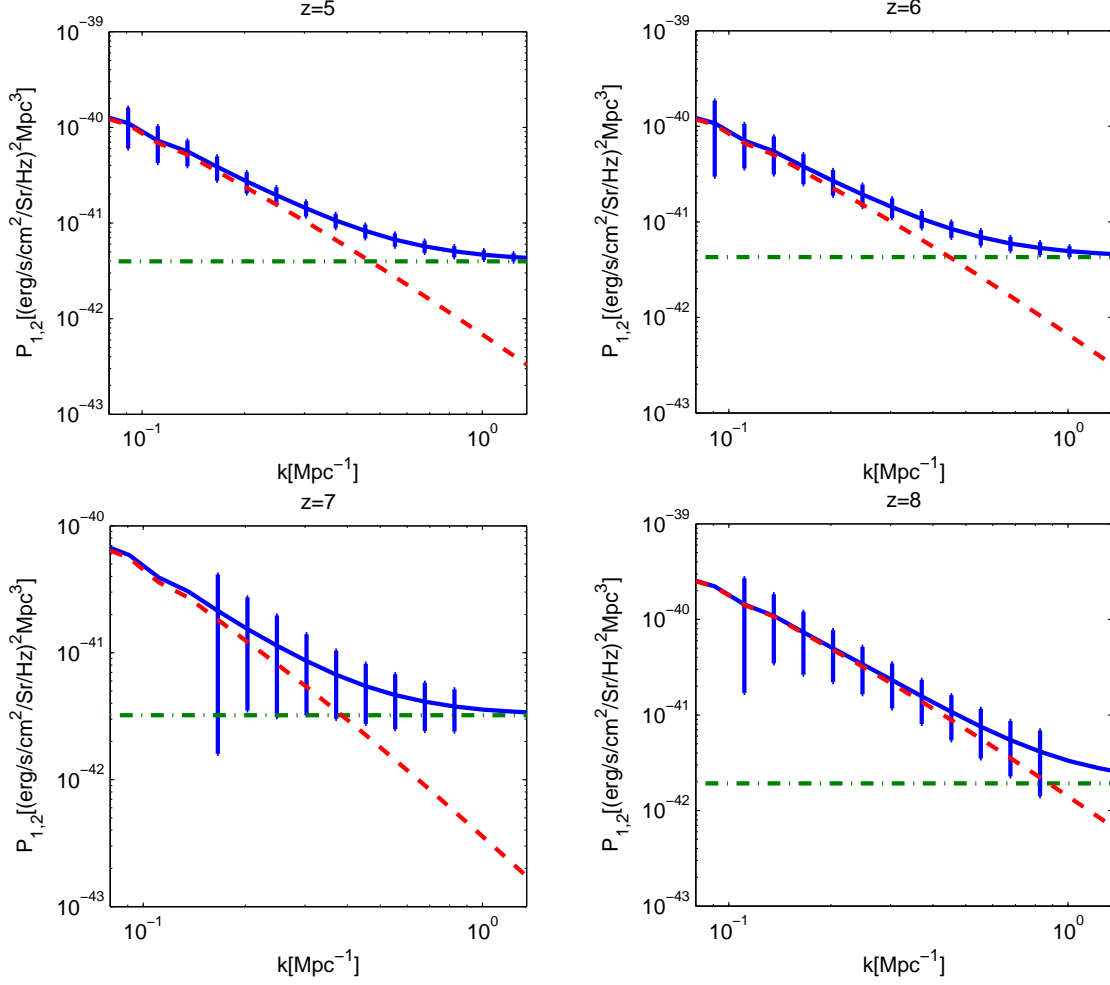


FIG. 2: The cross power spectrum of the OI($63\mu\text{m}$) and OIII($52\mu\text{m}$) lines at redshifts of $z = 5 - 8$. Bright sources which can be individually detected have been removed. The dashed line is the clustering component, the dot-dashed line is the shot-noise power spectrum due to the discrete nature of galaxies and the solid line is their sum. The error bars show the root-mean-square error on the cross power spectrum for a 10^6 second observation with SPICA. We assume that the survey is comprised of 256 adjacent pointings on the sky and has a depth of $\Delta z = 0.1(1 + z)$. In the $z = 5 - 7$ panels we have assumed that reionization occurred at a much higher redshift. In the $z = 8$ panel we have assumed that reionization occurred instantaneously at $z = 6$; this increases the signal to noise because it reduces the minimum mass of galaxies. The errors have been determined by averaging the cross power spectrum in bins of width $\Delta k = k/5$.

halos with virial radii corresponding to angles smaller than the pixels of the instrument we consider. Additionally, sub-halos which constitute more than $\approx 10\%$ of the parent halo are expected to sink to its center by dynamical friction in less than a Hubble time [42, 43]; this implies that each halo will most of the time have one dominant galaxy at its center and only much fainter satellites.

There is another argument which justifies our one pixel assumption for removing the detectable galaxies. For low redshift galaxies contributing to the bad line noise in the power spectrum, we find that the minimum mass of halos which have galaxies that can be directly

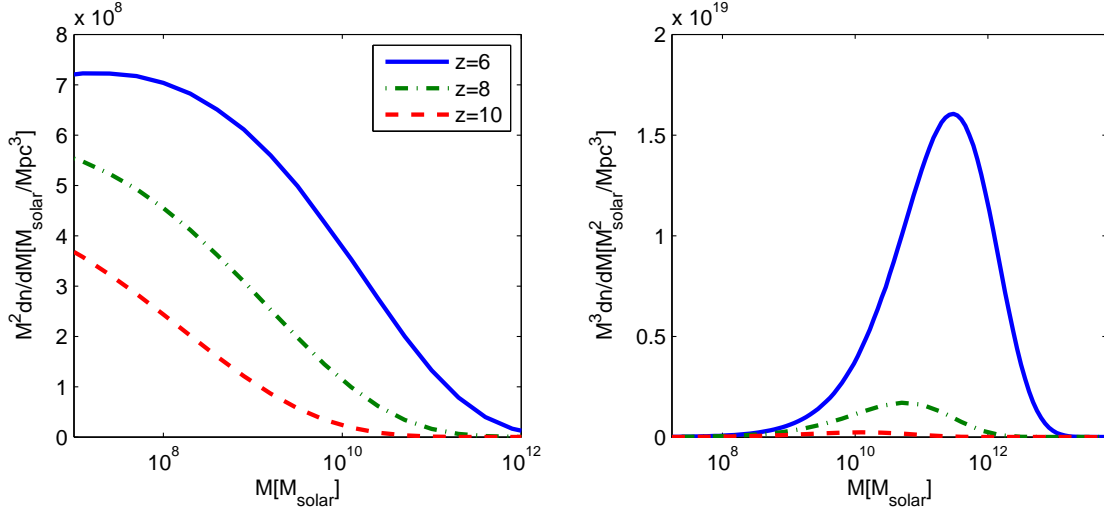


FIG. 3: The mass distributions $M^2 \frac{dn}{dM}$ (left) and $M^3 \frac{dn}{dM}$ (right) versus M at various redshifts. The area under the first is proportional to the contribution to the average line signal (see Eq. (9)) from the corresponding mass range, while for the second it is proportional to the contribution to the shot-noise power spectrum (see Eq. (12)). We see that most of the average signal and thus the clustering component of the cross power spectrum comes from low mass halos.

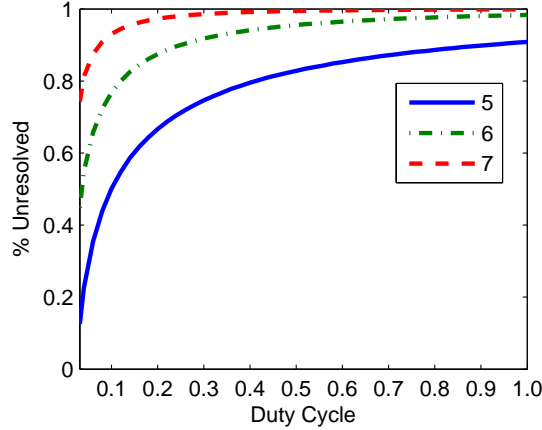


FIG. 4: The percentage of the average OI($63 \mu\text{m}$) line signal which originates from galaxies that are less than 3σ peaks in the noise versus duty cycle. We assume a 10^6s observation with 256 different pointings. As the duty cycle goes up there are more halos hosting fainter galaxies increasing the amount of signal which will come from galaxies which cannot be directly detected.

detected and removed is smaller than halos which host more than one galaxy. The number of galaxies per halo above this mass scales roughly linearly with halo mass [44]. Thus, if the galaxies are equally luminous in halos which host multiple galaxies, all of them can be directly detected and removed. When they are not equally luminous most of the signal will originate from the brighter galaxies which will be removed.

In all of our calculations we use the linear power spectrum computed with CAMB [45]. We expect the linear power spectrum to be a good approximation. The smallest scales probed in our examples are still in the linear regime at the redshifts of interest. On these scales we

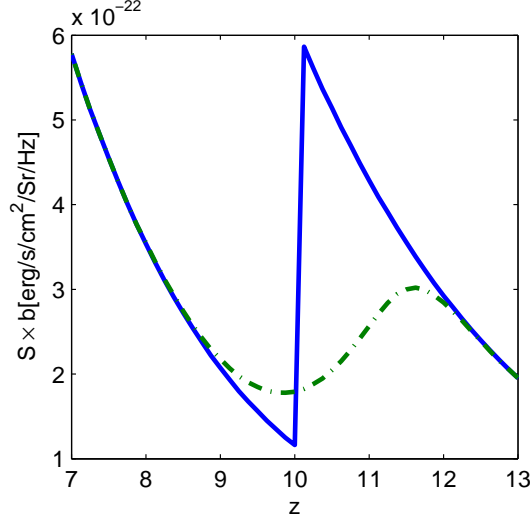


FIG. 5: The average OI($63\ \mu\text{m}$) line signal times the bias as a function of redshift. For the solid curve we have assumed that reionization occurs instantaneously at $z = 10$ and that the minimum mass of galaxies changes from the requirement that hydrogen cooling is efficient to the Jean’s mass after reionization. In the other curve, the change in minimum mass has been smoothed with an error function. While these may not be realistic reionization histories, this figure illustrates that one may probe the reionization history with the cross power spectrum. Though we have shown the cross power spectrum corresponding to reionization at $z = 10$, note that it may be difficult to observe this signal with SPICA.

may be in the nonlinear regime of the matter power spectra at lower redshifts which appear in the bad line noise terms. One way to approximate the nonlinear power spectrum is to use the so called Halo Model (see [46] and references therein). In this treatment, correlations are separated into two terms: the 1-halo term corresponding to correlations between matter in the same halo and the 2-halo term corresponding to correlations between matter in different halos. After removing bright sources we expect the signal to be coming from the center of halos. Thus, the 1-halo contribution to our cross power spectrum will originate only from the shot-noise power spectrum given in Eq. (12). The linear power spectrum should give a reasonable approximation to the 2-halo term.

We adopt fiducial values of the duty cycle and star formation efficiency of $\epsilon_{\text{duty}} = 0.1$ and $f_* = 0.1$ [41]. The total observation time is assumed to be 10^6 seconds. During this time we assume that 256 adjacent pointings are taken to provide a mosaic over an area of the sky. Increasing the number of pointings reduces the error in the power spectrum due to sample variance, including noise provided by bad lines, but increases the error due to the detector noise power spectrum since fewer photons are collected in each pointing. For the depth of the survey along the line of sight we assume $\Delta z = 0.1(1 + z)$. We assume that the cosmological evolution across this redshift range is negligible.

In Figure 2, we plot the OI($63\mu\text{m}$) and OIII($52\mu\text{m}$) cross power spectrum with error bars. For the plot at $z = 5, 6$ and 7 we have assumed that reionization occurred at a much higher redshift, such that the minimum mass of halos which host galaxies is determined from the Jeans mass in the photo-ionized IGM with a minimum virial temperature of 10^5K [22–27]. For the plot at $z = 8$ we assumed that reionization occurred instantaneously at $z = 6$ so

that the minimum mass of galaxies at the target redshift is set by the condition that there is efficient atomic hydrogen cooling with a minimum virial temperature of 10^4K [28, 29]. Because this corresponds to a smaller minimum mass there is more signal, improving the signal-to-noise ratio. In all of the plots we show the clustering and shot-noise components which make up the power spectrum. In all cases the clustering signal dominates on large scales. The error bars are much smaller for high k -values because they represent clustering on small scales and there are many more small scale regions to sample within a given survey volume.

The OI($145\mu\text{m}$) bad line for OI($63\mu\text{m}$) and the NII($122\mu\text{m}$) bad line for OIII($52\mu\text{m}$) originate from very nearby redshifts. Thus, the cross correlation of these could produce a spurious signal. However, we find that for our $z = 5 - 6$ examples all of the galaxies emitting this spurious signal could be located with the CII($158\mu\text{m}$) line and removed. For the $z = 7 - 8$ examples one may need to measure and subtract away some of the spurious signal as discussed above. This was not considered for Figure 2 and could slightly degrade the constraints on the cross power spectrum at these redshifts.

Figure 3 shows $M^2 \frac{dn}{dM}$ and $M^3 \frac{dn}{dM}$ versus M . The area under the first distribution is proportional to the contribution to the average signal from the corresponding halo mass range. Similarly, for the second function the area under the curve is proportional to the contribution to the shot-noise power spectrum. Fainter sources contribute more to the clustering signal because of their great numbers. By contrast, the shot-noise signal originates mainly from bright sources. If the brightest sources are removed, then the shot-noise signal should be substantially reduced while the clustering signal remains relatively unchanged. Owing to the hierarchical nature of structure formation in the universe more matter will be located in smaller halos at higher redshifts.

Figure 4 shows the fraction of the average OI($63\mu\text{m}$) signal which originates from lines that would be detected at less than 3σ significance for different values of the duty cycle. The average signal does not depend on the duty cycle because at lower values, the brightness of galaxies in our model goes up by the same factor that reduces the number of active galaxies. Thus, our technique is particularly effective if the duty cycle is high. This results in a higher number of fainter galaxies which would be harder to detect directly, but just as easy statistically using the cross power spectrum.

Figure 5 shows the average signal times the bias as a function of redshift for different reionization histories. We show one line assuming that reionization is sudden and that M_{min} changes instantaneously and a line which smooths the transition of M_{min} with an error function. For the smoothed case, the minimum mass of halos hosting galaxies is given by,

$$M_{\text{min}}(z) = \left(M_1 - \frac{(M_1 - M_2)}{2} [1 + \text{erf}(z - z_r)] \right) \left(\frac{10}{1 + z} \right)^{3/2}, \quad (31)$$

where $M_1 = 3 \cdot 10^9 M_{\odot}$, $M_2 = 10^8 M_{\odot}$, and the redshift of reionization $z_r = 10$. While these are not necessarily realistic reionization histories, they illustrate that the minimum mass of halos which host galaxies could be detected with the cross correlation technique. It may be difficult to observe the cross power spectrum at $z = 10$. If reionization occurs later it will be easier to study. If many different lines are used one may be able to probe higher redshifts than those shown in Figure 2.

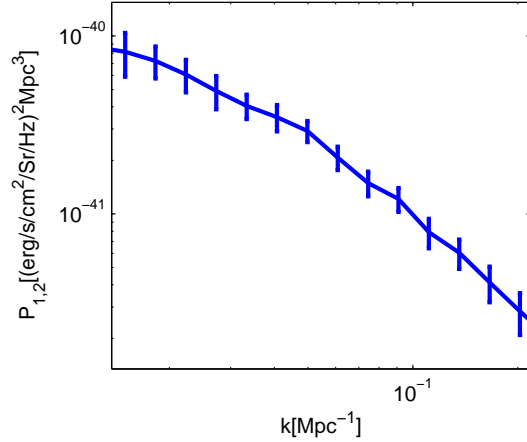


FIG. 6: The cross power spectrum of CO(8-7) and 21-cm galaxy line emission at $z = 3$. The shot-noise power spectrum is negligible for the values of k shown. The error bars show the root-mean-square error on the cross power spectrum for a 10^6 second observation with CCAT and a separate 10^6 second observation with our hypothetical 21cm interferometer. We assume a survey depth of $\Delta z = 0.1(1 + z)$.

IV. CROSS-CORRELATING CO LINES WITH 21-CM EMISSION

A. Instruments

As another example, we consider cross correlating CO line emission measured with a large ground based telescope and 21-cm line emission from neutral hydrogen in galaxies measured with an interferometer optimized for frequencies corresponding to post-reionization redshifts. As discussed above, in order to measure fluctuations in line emission, one must first fit and subtract away the bright foreground signal. Because they will have completely different sources of foreground emission, cross correlating CO and 21-cm line emission could eliminate any residual foregrounds if they are present after this subtraction process.

The Cornell Caltech Atacama Telescope (CCAT) is a large sub-mm telescope to be built at high altitude in the Atacama region of northern Chile [20]. It will be a 25 meter telescope with a 10 arcminute field of view. We consider a hypothetical instrument which takes spectra of 1000 adjacent diffraction limited beams simultaneously. We assume spectrometers with resolving power of $R = \nu/\Delta\nu = 1000$ and background limited sensitivity on CCAT. Specifically, we use the numbers listed in Figure 6 of Ref. [47].

For the 21cm experiment, we consider a hypothetical interferometer which is similar to the Murchison Widefield Array (MWA) [6], but optimized to observe 21-cm emission at a redshift of $z=3$. We assume an array of 500 tiles each consisting of 16 dipoles with an effective area of $A_e = 2.8\text{m}^2$ per tile.

B. Results

To calculate the CO line signal we use the approach discussed in §3.2. As in the SPICA example, we assume a duty cycle of $\epsilon_{\text{duty}} = 0.1$ and star formation efficiency of $f_* = 0.1$.

After reionization 21-cm emission is expected to come from self-shielded neutral hydrogen in galaxies [15, 16]. After reionization, the difference between the average observed 21-cm brightness temperature from redshift z and the CMB temperature today is described by

$$\bar{T}_b \approx 26\bar{x}_H \left(\frac{\Omega_b h^2}{0.022} \right) \left(\frac{0.15}{\Omega_m h^2} \frac{1+z}{10} \right)^{1/2} \text{ mK}, \quad (32)$$

where \bar{x}_H is the global mass-averaged neutral hydrogen fraction. Observations have shown that out to $z \approx 4$ the cosmological density parameter of HI is $\Omega_{\text{HI}} \approx 10^{-3}$ [48]. This corresponds to a mass-averaged neutral fraction of a few percent. For our calculations we assume a value of $\bar{x}_H = 0.02$. In the context of the formalism discussed above, \bar{T}_b is the average line signal after converting to units of (ergs/s/cm²/Hz/Sr) with the Rayleigh-Jeans Law. With this quantity we can also calculate the shot-noise power spectrum as we did with Eq. (12). For this calculation, we assume that the 21-cm flux originating from dark matter halos above M_{min} is proportional to their mass. The shot-noise power spectrum is lower than our previous example because we have emission from all halos above the minimum mass as opposed to a smaller fraction set by the duty cycle.

The noise power spectrum is given by

$$P_{\text{noise}}(k \sin \theta) = D_A^2 \tilde{y} \left(\frac{\lambda^2 T_{\text{sys}}}{A_e} \right)^2 \frac{1}{t_0 n(k \sin \theta)}, \quad (33)$$

where $\lambda = 21\text{cm} \times (1+z)$ is the observed wavelength, T_{sys} is the system temperature of the interferometer, A_e is the effective area of each tile, t_0 is the total observing time, and $n(k \sin \theta)$ is the number density of baselines where $k = |\mathbf{k}|$ and θ is the angle between \mathbf{k} and the line of sight. The baseline density $n(k \sin \theta)$ depends on the geometrical configuration of the 500 antenna tiles. We have assumed a distribution of tiles with constant density within the innermost 8.9m and which falls off as r^{-2} out to 330m. We assume that $T_{\text{sys}} = T_{\text{sky}} + T_{\text{inst}}$ where the sky temperature $T_{\text{sky}} = 260 [(1+z)/9.5]^{2.55}$ [49], and that the instrumental temperature is $T_{\text{inst}} = 100\text{K}$. For a derivation of the expression which gives the noise power spectrum see Ref. [13].

In Figure 6 we plot the cross power spectrum of CO(8-7) and 21-cm line emission at $z = 3$. We show the error bars corresponding to an observation lasting 10^6 seconds for each instrument and covering the field of view of one primary beam, $\Omega = \lambda^2/A_e = 0.25$ Sr, of our MWA-like interferometer.

V. DISCUSSION AND CONCLUSIONS

In this paper, we have developed a formalism for measuring the cross power spectrum of line emission from galaxies. Cross correlating the flux fluctuations in different lines from the same galaxies removes the contaminating signal from other “bad lines.” We demonstrated that it is possible to statistically measure the line fluctuation signal from undetected galaxies at some target redshift. The distinct difference and advantage of this technique compared to traditional galaxy surveys is that the signal originates from *all* sources of line emission rather than just the high signal-to-noise peaks in the data. In this way it is possible to study large populations of faint galaxies in a reasonable amount of observing time. Even though individual galaxies will be difficult to detect, their large numbers contribute significantly to

the total signal. The relative contributions of different mass ranges to the clustering signal can be seen in Figure 3. At high redshifts, the faintest galaxies produce the most signal per logarithmic mass interval.

The cross power spectrum of line emission measures the product of the cosmic matter power spectrum, the average signal coming from a pair of lines and the luminosity weighted bias of the source galaxies. For the standard set of cosmological parameters, one knows the theoretical value of the matter power spectrum. The cross power spectrum then gives the product of the two average line signals with the bias squared. The shot-noise component of the cross power spectrum depends on the duty cycle while the clustering component does not. This allows an estimation of the duty cycle by comparing the cross power spectrum at low k -values where clustering dominates to high k values where the shot-noise component dominates.

We demonstrated this technique by showing that atomic and ionic fine structure lines from galaxies could be cross correlated using the proposed SPICA mission. We have found that for OI($63\mu m$) and OIII($52\mu m$) and an observation lasting a total of 10^6 seconds, the cross power spectrum of sources too faint to be directly detected can be measured accurately out to $z \approx 8$. This is important because depending on the duty cycle, most of the line emission signal originates from galaxies which cannot be detected otherwise.

The cross power spectrum at these redshifts allows one to measure the total emission in O and N lines from a large sample of faint galaxies as a function of redshift. This information would constrain the evolution of galaxy properties such as metallicity and star formation rate. It also constrains the bias and duty cycles of the source galaxies. Finally, the value of the average signal is sensitive to the minimum mass of galaxies, and so the evolution in the average line signal could constrain the reionization history.

We also consider an example where we cross correlate the CO and 21-cm line emission from galaxies measured with CCAT and an interferometer similar in scale to MWA, but optimized for post-reionization redshifts. As in the SPICA example, this would yield important information about the evolution of CO emission from galaxies over cosmic time. Because we expect the foregrounds in CO and 21-cm observations to be uncorrelated, cross correlation could eliminate spurious residual foreground emission if any remained after the removal process. Of course, one could also cross correlate different lines, such as the various CO lines and CII($158\mu m$), with an instrument like CCAT alone.

In our calculations we have assumed that the foregrounds are smooth in frequency and can be removed perfectly, leaving only the fluctuations due to line emission and detector noise. If the foregrounds vary rapidly as a function of angle on the sky it may only be possible to measure k -modes along the line of sight.

The cross correlation technique is general and may be used for many different lines (such as those listed in Table I). It will be most useful for instruments which have a large field of view, but cannot detect individual faint sources effectively. Additional angular or spectral resolution will provide access to fluctuations on smaller scales, but will not improve the accuracy of the cross power spectrum on large scales.

Acknowledgments

We thank Mark Dijkstra and Jonathan Pritchard for useful comments. We also thank the referee, Asantha Cooray, for helpful suggestions. This work was supported in part by

-
- [1] J. Binney and M. Merrifield, *Galactic astronomy* (Princeton University Press, 1998).
 - [2] <http://www.sdss.org/>.
 - [3] <http://www2.aao.gov.au/2dFGRS/>.
 - [4] <http://deep.berkeley.edu/marc/deep/index.html>.
 - [5] <http://www.oamp.fr/virmos/vvds.htm>.
 - [6] <http://www.haystack.mit.edu/ast/arrays/mwa>.
 - [7] <http://www.lofar.org>.
 - [8] <http://www.astro.berkeley.edu/dbacker/EoR>.
 - [9] <http://web.phys.cmu.edu/past>.
 - [10] <http://www.skatelescope.org>.
 - [11] M. F. Morales, *Astrophys. J.* **619**, 678 (2005).
 - [12] X.-M. Wang, M. Tegmark, M. Santos, and L. Knox, *Astrophys. J.* **650**, 529 (2006).
 - [13] M. McQuinn, O. Zahn, M. Zaldarriaga, L. Hernquist, and S. R. Furlanetto, *Astrophys. J.* **653**, 815 (2006).
 - [14] A. Liu, M. Tegmark, J. Bowman, J. Hewitt, and M. Zaldarriaga, *Mon. Not. Roy. Astron. Soc.* **398**, 401 (2009), arXiv:astro-ph/0903.4890.
 - [15] J. S. B. Wyithe and A. Loeb, *Mon. Not. Roy. Astron. Soc.* **397**, 1926 (2009).
 - [16] A. Loeb and J. S. B. Wyithe, *Physical Review Letters* **100**, 161301 (2008), arXiv:astro-ph/0801.1677.
 - [17] T. Chang, U. Pen, K. Bandura, and J. B. Peterson, *Nature (London)* **466**, 463 (2010).
 - [18] K. Sigurdson and S. R. Furlanetto, *Physical Review Letters* **97**, 091301 (2006), arXiv:astro-ph/0505173.
 - [19] B. Swinyard, T. Nakagawa, P. Merken, P. Royer, T. Souverijns, B. Vandenbussche, C. Waelkens, P. Davis, J. Di Francesco, M. Halpern, et al., *Experimental Astronomy* **23**, 193 (2009).
 - [20] <http://www.submm.org/>.
 - [21] E. Komatsu, K. M. Smith, J. Dunkley, C. L. Bennett, B. Gold, G. Hinshaw, N. Jarosik, D. Larson, M. R.olta, L. Page, et al., *ArXiv e-prints* (2010), arXiv:astro-ph/1001.4538.
 - [22] A. Mesinger and M. Dijkstra, *Mon. Not. Roy. Astron. Soc.* **390**, 1071 (2008).
 - [23] G. Efstathiou, *Mon. Not. Roy. Astron. Soc.* **256**, 43P (1992).
 - [24] A. A. Thoul and D. H. Weinberg, *Astrophys. J.* **465**, 608 (1996).
 - [25] L. Hui and N. Y. Gnedin, "Mon. Not. Roy. Astron. Soc." **292**, 27 (1997).
 - [26] S. Wyithe and A. Loeb, *Nature* **441**, 332 (2006).
 - [27] P. R. Shapiro, M. L. Giroux, and A. Babul, *Astrophys. J.* **427**, 25 (1994).
 - [28] D. Babich and A. Loeb, *Astrophys. J.* **640**, 1 (2006), arXiv:astro-ph/0509784.
 - [29] Z. Haiman, M. J. Rees, and A. Loeb, *Astrophys. J.* **476**, 458 (1997), arXiv:astro-ph/9608130.
 - [30] R. K. Sheth, H. J. Mo, and G. Tormen, *Mon. Not. Roy. Astron. Soc.* **323**, 1 (2001).
 - [31] <http://science.nrao.edu/alma/index.shtml>.
 - [32] D. J. Fixsen, E. Dwek, J. C. Mather, C. L. Bennett, and R. A. Shafer, *Astrophys. J.* **508**, 123 (1998), arXiv:astro-ph/9803021.
 - [33] J. Zmuidzinas, *Appl. Opt.* **42**, 4989 (2003).
 - [34] A. Loeb, *JCAP* **4**, 21 (2008), 0801.0441.

- [35] R. C. Kennicutt, Jr., *Annual Review of Astronomy and Astrophysics* **36**, 189 (1998), arXiv:astro-ph/9807187.
- [36] M. Righi, C. Hernández-Monteagudo, and R. A. Sunyaev, *Astronomy and Astrophysics* **489**, 489 (2008), arXiv:astro-ph/0805.2174.
- [37] S. Malhotra, M. J. Kaufman, D. Hollenbach, G. Helou, R. H. Rubin, J. Brauher, D. Dale, N. Y. Lu, S. Lord, G. Stacey, et al., *Astrophys. J.* **561**, 766 (2001), arXiv:astro-ph/0106485.
- [38] A. Weiß, F. Walter, and N. Z. Scoville, *Astronomy and Astrophysics* **438**, 533 (2005), arXiv:astro-ph/0504377.
- [39] P. Panuzzo, N. Rangwala, A. Rykala, K. G. Isaak, J. Glenn, C. D. Wilson, R. Auld, M. Baes, M. J. Barlow, G. J. Bendo, et al., *Astronomy and Astrophysics* **518**, L37+ (2010), 1005.1877.
- [40] A. Loeb, R. Barkana, and L. Hernquist, *Astrophys. J.* **620**, 553 (2005), arXiv:astro-ph/0403193.
- [41] D. P. Stark, A. Loeb, and R. S. Ellis, *Astrophys. J.* **668**, 627 (2007), arXiv:astro-ph/0701882.
- [42] A. R. Wetzel, J. D. Cohn, and M. White, *Mon. Not. Roy. Astron. Soc.* **395**, 1376 (2009), arXiv:astro-ph/0810.2537.
- [43] A. R. Wetzel and M. White, *Mon. Not. Roy. Astron. Soc.* **403**, 1072 (2010), arXiv:astro-ph/0907.0702.
- [44] J. S. Bullock, R. H. Wechsler, and R. S. Somerville, *Mon. Not. Roy. Astron. Soc.* **329**, 246 (2002), arXiv:astro-ph/0106293.
- [45] <http://camb.info/>.
- [46] A. Cooray and R. Sheth, *Physics Reports* **372**, 1 (2002), arXiv:astro-ph/0206508.
- [47] C. M. Bradford, J. E. Aguirre, J. J. Bock, L. Earle, J. Glenn, H. Inami, P. R. Maloney, H. Matsuhara, B. J. Naylor, H. T. Nguyen, et al., in *Astronomical Society of the Pacific Conference Series*, edited by D. C. Lis, J. E. Vaillancourt, P. F. Goldsmith, T. A. Bell, N. Z. Scoville, & J. Zmuidzinas (2009), vol. 417 of *Astronomical Society of the Pacific Conference Series*, pp. 341–+.
- [48] J. X. Prochaska, S. Herbert-Fort, and A. M. Wolfe, *Astrophys. J.* **635**, 123 (2005).
- [49] A. E. E. Rogers and J. D. Bowman, *The Astronomical Journal* **136**, 641 (2008).

Appendix A: Error on cross power spectrum

The error on an estimate for the cross power spectrum at a particular wave-vector is given by,

$$\delta P_{1,2}^2 = \langle \hat{P}_{1,2}^2 \rangle - \langle \hat{P}_{1,2} \rangle^2 = \left\langle \frac{V^2}{4} (f_{\mathbf{k}}^{(1)} f_{\mathbf{k}}^{(2)*} + f_{\mathbf{k}}^{(1)*} f_{\mathbf{k}}^{(2)})^2 \right\rangle - P_{1,2}^2, \quad (\text{A1})$$

where V is the survey volume and $f_{\mathbf{k}}$ is the Fourier amplitude defined in Eq. (13) with superscripts denoting the target lines being cross correlated. For each target line we break up $f_{\mathbf{k}}$ into terms corresponding to those in Eq. (1). Plugging Eq. (14) into Eq. (A1) and expanding we are left with the sum of many products of four Fourier modes, many of which are not correlated and vanish. We are only left with products of Fourier amplitudes that are correlated: detector noise with itself, the bad lines' fluctuations with themselves and the target lines' fluctuations with themselves and one another. We then only need to calculate the average value of these various products.

The terms involving detector noise are easily calculated by changing the integral in

Eq. (13) into a sum. It follows that,

$$\langle V f_{\mathbf{k}}^{n1} f_{\mathbf{k}}^{n1*} \rangle = P_{\text{noise}} = \sigma_n^2 V_{\text{pix}}, \quad (\text{A2})$$

where σ_n^2 is the variance of the noise in units of ergs/s/cm²/Hz/Sr in a single pixel and V_{pix} is the survey volume corresponding to each pixel.

The Fourier amplitudes corresponding to the bad lines are given by

$$f_{\mathbf{k}}^{B1} = \bar{B}_1 \bar{b}_1 \int d^3 \mathbf{r} \delta(\mathbf{r}_o + d_1 \hat{\mathbf{k}} + \mathbf{r}'_1) W(\mathbf{r}) e^{i\mathbf{k} \cdot \mathbf{r}}, \quad (\text{A3})$$

where $\mathbf{r}'_1 = c_{x1} x \hat{\mathbf{i}} + c_{y1} y \hat{\mathbf{j}} + c_{z1} z \hat{\mathbf{k}}$. We change integration variables from (x, y, z) to $(x'_1 = c_{x1} x, y'_1 = c_{y1} y, z'_1 = c_{z1} z)$, and proceed as we did in Eqs. (15)-(19). We find,

$$\langle V f_{\mathbf{k}}^{B1} f_{\mathbf{k}}^{B1*} \rangle = \bar{B}_1^2 \bar{b}_1^2 \frac{P(\mathbf{k}'_1, z_1)}{(c_{x1} c_{y1} c_{z1})}, \quad (\text{A4})$$

where $\mathbf{k}'_1 = \frac{k_x}{c_{x1}} \hat{\mathbf{i}} + \frac{k_y}{c_{y1}} \hat{\mathbf{j}} + \frac{k_z}{c_{z1}} \hat{\mathbf{k}}$. The c 's in these equations reflect the stretching and squeezing of the data cube at the redshifts of the spurious lines due to the redshift dependence of the angular diameter distance and frequency per comoving interval as described above.

It is also necessary to calculate terms like,

$$\begin{aligned} V^2 \langle f_{\mathbf{k}}^{S1*} f_{\mathbf{k}}^{S1*} f_{\mathbf{k}}^{S2} f_{\mathbf{k}}^{S2} \rangle = \\ V^2 \frac{1}{(2\pi)^{12}} \int \int \int \int d^3 \mathbf{k}_1 d^3 \mathbf{k}_2 d^3 \mathbf{k}_3 d^3 \mathbf{k}_4 W(\mathbf{k}_1 - \mathbf{k}) W(\mathbf{k}_2 - \mathbf{k})^* W(\mathbf{k}_3 - \mathbf{k})^* W(\mathbf{k}_4 - \mathbf{k}) \\ \times \bar{S}_1^2 \bar{S}_2^2 \bar{b}^4 \langle \delta(\mathbf{k}_1) \delta(\mathbf{k}_2)^* \delta(\mathbf{k}_3)^* \delta(\mathbf{k}_4) \rangle e^{-i(\mathbf{k}_1 - \mathbf{k}_2 - \mathbf{k}_3 + \mathbf{k}_4) \cdot \mathbf{r}_o} = 2 \bar{S}_1^2 \bar{S}_2^2 \bar{b}^4 P(\mathbf{k}), \end{aligned} \quad (\text{A5})$$

where to calculate this integral we have used Wick's theorem $\langle \delta_1 \delta_2 \delta_3 \delta_4 \rangle = \langle \delta_1 \delta_2 \rangle \langle \delta_3 \delta_4 \rangle + \langle \delta_1 \delta_3 \rangle \langle \delta_2 \delta_4 \rangle + \langle \delta_1 \delta_4 \rangle \langle \delta_2 \delta_3 \rangle$. We also used Eq. (18) and the fact that for a large survey $|W(\mathbf{k}' - \mathbf{k})|^2 \approx (2\pi)^3 \delta^D(\mathbf{k}' - \mathbf{k})/V$.

Putting all of this together we find,

$$\delta P_{1,2}^2 = \frac{1}{2} (P_{1,2}^2 + P_{1\text{total}} P_{2\text{total}}), \quad (\text{A6})$$

where $P_{1\text{total}}$ is the total power spectrum corresponding to the first line being cross correlated,

$$P_{1\text{total}} = \bar{S}_1^2 \bar{b}^2 P(\mathbf{k}, z_{\text{target}}) + P_{\text{noise1}} + \bar{B}_1^2 \bar{b}_1^2 \frac{P(\mathbf{k}'_1, z_1)}{(c_{x1} c_{y1} c_{z1})} + \bar{B}_2^2 \bar{b}_2^2 \frac{P(\mathbf{k}'_2, z_2)}{(c_{x2} c_{y2} c_{z2})} \dots \quad (\text{A7})$$

The equation corresponding to the second line being cross correlated is exactly the same, but of course contains the noise at a different frequency and will have bad lines at different redshifts. There will also be a shot-noise power spectrum for each clustering spectrum included above, which was not written to avoid a cumbersome equation.